Progress in Additive Manufacturing
https://doi.org/10.1007/s40964-024-00570-8

FULL RESEARCH ARTICLE

Investigating enhanced interfacial adhesion in multi-material filament 3D printing: a comparative study of t and Mickey Mouse geometries

M. Frascio[1] · A. Zafferani[1] · M. Monti[1] · M. Avalle[1]

Received: 3 October 2023 / Accepted: 20 January 2024

Abstract
In this study, a novel design to enhance interfacial adhesion in multi-material components produced through filament 3D printing techniques is presented. Multi-material additive manufacturing often faces challenges related to poor chemical affinity between polymers and physical discontinuities between component sub-parts. To address these issues, an interface geometry that leverages both diffusion and mechanical adhesion mechanisms to facilitate interlocking is proposed. The performance of the widely used T-shaped geometry, as per existing literature, with a newly introduced Mickey Mouse lobate modified shape is compared. Additionally, the linear butt interface, which relies solely on chemical diffusion is investigated. For the study, Polylactic Acid and Polyethylene Terephthalate as the material pairs was selected. The findings underscore the significant impact of interface geometry on the mechanical properties of multi-material components. Using the ultimate tensile strength of the standard ISO 527-2 specimen as a reference, a butt interface results in a residual strength of 60% for homogeneous materials, but only 10% for heterogeneous materials. The adverse impact of the heterogeneous materials configuration was alleviated by the interfaces, leading to an enhancement of 7% and 58% for the Mickey Mouse and T geometries, respectively. While the Mickey Mouse geometry effectively reduces stress concentrations, it falls short of achieving the desired improvement in multi-material adhesion between parts. This outcome suggests the necessity of further research, particularly towards optimizing the proposed geometry for enhanced performance.

Keywords Multi-material · Additive manufacturing · Fused filament fabrication · Fused deposition modeling · Adhesion · Interface

1 Introduction

The technological development of Additive manufacturing [1] (AM) and of multi-material additive manufacturing (MMAM) [2, 3] processes made possible to produce structurally functionalized engineered components bypassing the need to carry out secondary operations such as gluing and welding [4–9].

Nature, as a 'design' teacher, shows us how it can be advantageous to create combinations of compositional and functional gradations of materials and structures, as seen, for example, in human bones and fish scales that combine stiffness and damage resistance [10, 11]. Such behavior is made possible by the combination of hierarchical cellular structures and material gradation that has been engineered for tailoring specific properties. For example, stiffness gradation can be used to prevent or delay delamination in laminated materials [12–14] or nanoscale tessellation can be used to increase toughness [15, 16] and crack propagation resistance [17, 18]. Another research field in which MMAM is playing a crucial role is the functionalization of components using composite materials designed to modify the physical properties of the base polymer [19–23]. These composite materials are created by selecting the type and percentage of reinforcing material to optimize a specific physical property for the application. For example, electrical resistance should be as low as possible to create integrated electrical circuits [24] or embedded sensors [25, 26], while for heating elements, it should be sufficient to generate the necessary heat through the Joule effect [7]. It can be used also for 4D printing, i.e., memory shape materials [27–29].

As seen, research on MMAM is mainly focused on its constructive potential and the new applications it offers

✉ M. Frascio
mattia.frascio@unige.it

[1] Università Di Genova, Via Balbi 5, 16100 Genoa, Italy

Published online: 29 February 2024

compared to subtractive manufacturing or single-material AM. As a matter of fact, the distinguishing feature of AM, especially when it comes to FDM, of progressive addition of material allows to produce elements with complex shapes, such as cavities or undercuts. Fabrication of form-fit joints, e.g., snap-fit joints, is an illustrative application of how AM processes can overcome the limitations in terms of geometrical complexity encountered with the traditional methods of injection molding and extrusion [30]. Moreover, in this instance, MMAM unlike single-material AM can be a valid technique to develop potential improvements. In particular, producing the beam of the clip with a composite tied with a thin metal layer may increase the strength of these joints and facilitate the assembly phase by taking advantage of dissimilar thermal expansions of the different materials of the parts [31].

Although the use of multi-material processes is widely increasing, it has to be acknowledged that in comparison to existing literature studies on AM regarding material modelling [32–34] and component characterization [35–38], the effect of the MMAM process on the final mechanical properties is still relatively underexplored. Moreover, is worth noting that, according to the previously reported articles, in MMAM at each material interface the currently adopted interface is traceable to a butt joint. This work aims are to assess the relevance of the material interface on the mechanical properties of a MMAM-ed component, also in relation to the material interface geometry, to evaluate if it should be taken in account as one of the design factors in the design for additive manufacturing DfAM.

2 Materials interface design

In the MMAM, at the interface between the two materials, there are several factors that can influence strength in addition to the geometry [39], such as the overall contact surface, the compatibility between different materials, and the thermal cycle created by the nozzle during polymer deposition.

Most of the existing studies are focused on determining whether a mechanical interface geometry that generates an interlocking mechanism performs better than one based on simple chemical diffusion between materials. More specifically, when two different materials are joined through FDM process, the formation of interfacial bond starts when the two polymers come into contact. The process of the intermolecular diffusion is activated by the high temperature of the materials and the polymer chains begin to move across the contact area. It has to be noted that the deposition of molten material on the previously extruded filaments allow the temperature of the overall process to stay around the same value, which enables the development of the interface bond [40]. However, it has been proven that in the case of polymers with low chemical affinity the adhesion force between them is not sufficient on its own, therefore an interlocking interface is necessary to confer a more robust bond, as it allows the coalescence forces to be combined with the macroscopic mechanical ones [41].

To assess the effect of the only interface, i.e. the effect of the chemical diffusion, the butt joint interface (Fig. 1a) was selected as it is a characterization method validated in adhesive joint testing [42].

Other two interfaces were investigated adding a geometrical locking effect, a T shape (Fig. 1b), which, according to literature, appears to be one of the best performing in terms of mechanical strength [41, 43, 44] and a modified T-lobed shape, Mickey-Mouse MM shape (Fig. 1c). The reason why the latter is introduced, is to overcome the problems encountered with the former interface. On one hand, sharp edges of the T-shape can generate stress concentrations due to the notch effect, on the other hand, its undercuts could be difficult to fabricate if not with additive techniques. As a matter of fact, Mickey Mouse geometry is proposed as an adjustment of the T-shaped one, making the upper wings more rounded and leaving the core of the section almost unchanged. In engineering this shape is not brand-new, since already used in some applications, as sheets glass milling. When manufacturing glass doors, MM-shaped notches are milled to make hinge slots which do not lead to excessive stress concentrations during the hypothetical following process of tempering.

The dimensioning of the T and MM shapes (Fig. 2) were optimized combining the results of works on mechanical interfaces shape optimization [41, 43, 45], dimensioning for printability [46, 47] and industrial state of the art for dissimilar material interfaces.

To be specific, the dimensions of Mickey Mouse geometry were adapted starting from the actual drawings of hinge slots milled in sheets glass [48], logically modified and scaled to make them comparable with the T shape proportions that can be detected in literature. However, in the first attempt to print specimens, material gaps were obtained near the interface line. The underlying motivation lies in

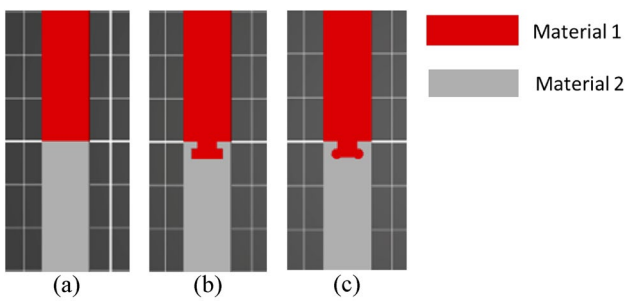

Fig. 1 Investigated interfaces

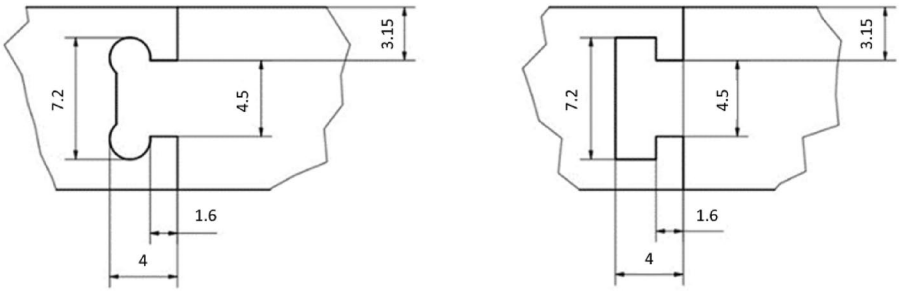

Fig. 2 T and MM shapes dimensions (units in mm)

the fact that both the dimensions of the geometry and the thickness of the samples were not a multiple of the width of the extruded filament. Consequently, all the dimensions were adjusted acknowledging that the width of the filament is 0.45 mm. This piece of data has been selected through the Slicing software PrusaSlicer [49] as the right compromise between a correct printing resolution and a not too slow production taking into consideration that the diameter of the printer nozzle is 0.4 mm and the height of each layer of deposited material is 0.2 mm.

The interfaces were inserted initially in the tensile test specimens (Fig. 3) from the normative UNI EN ISO 527-2:2012, geometry 1A. Taking in account the principles of the Design for Additive Manufacturing (DfAM) and the guidance of the National Institute of Standards and Technology NIST for the applicability of existing materials testing standards for additive manufacturing Materials [50], the specimens dimensioning was thereafter modified with a width of 10.8 mm, i.e., 24 times the filament. It was possible to deviate from the dimensions expressed in the normative as this investigation does not focus on the characterization of plastic materials, but on the analysis of the effect of the proposed geometries. As a matter of fact, the width of all the specimens was reshaped since otherwise certain samples would have had a different resistant section from the others, making the comparison inaccurate.

3 Material and methods

In this section the materials used in this work are reported and the characterization methods implemented to carry out the experimental tests are described in detail.

The selected base material was the polyethylene terephthalate PET manufactured by ICE filaments, Belgium [51], the second material was polylactic acid PLA manufactured by SUNLU, CA, US [52], provided as 1.75 mm diameter spool.

These polymers were selected following a compatibility study based on the carried-out investigations in literature. PLA/PET combination represents an excellent compromise between rigidity and flexibility, but without being characterized by completely different behaviors or a lower chemical affinity in comparison to other combinations [53]. PLA is known to be one of the most widely used polymers in extrusion-based 3D printing techniques due to its printability and good biological and mechanical properties, such as high tensile strength [54]. PET, on the other hand, mainly used in clothing and packaging applications, is tenacious, but not as rigid as PLA [55], therefore it gives the right balance to the PLA/PET couple.

The specimens realized, at least 3 each combination, were:

- UNI EN ISO 527-2:2012 standard 1A, compliant to DfAM, geometry PET
- UNI EN ISO 527-2:2012 standard 1A, compliant to DfAM, geometry PLA
- UNI EN ISO 527-2:2012 with each interface geometry, mono-material PLA (dark and light grey)
- UNI EN ISO 527-2:2012 with each interface geometry, mono-material PET (red and white)
- UNI EN ISO 527-2:2012 with each interface geometry, multi-material PET-PLA (red and light grey)

The last combination is investigated in the PET for the male part and PLA for the female part configuration. The standard 1A geometry, compliant to DfAM, is used to assess the base material properties according to the printing setup. The mono-material is used to isolate the effect of the

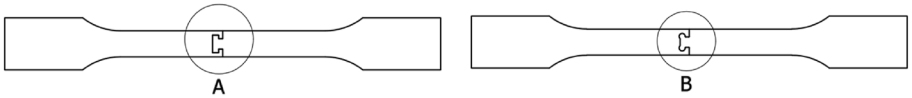

Fig. 3 T shape (**A**) and MM shape (**B**) in the 1A geometry from the UNI EN ISO 527–2:2012

interface, the multi-material is used to investigate the combined effect of the interface and of the materials.

Specimens were manufactured using a PRUSA Original Prusa i3 MK3 upgraded with the MMU2S kit (Multi Material Upgrade 2S) by PRUSA, Czech Republic [49]. Printing settings were optimized from literature [56–62] and experimental tests and then kept the same for all the configurations to prevent cross-interaction effect of the parameters on the tests results.

In particular, the infill density and the deposition pattern are respectively 100% and straight aligned, while the selected layup is unidirectional, therefore with the layers deposited all with the same orientation. Moreover, the position of the sample on the print bed with an infill angle of 90° allows the fibres to be aligned in parallel with the load direction. Several studies have shown that in this configuration it is possible to obtain more tenacity and resistance [63]. Furthermore, the upper and lower layers are omitted since they are only an aesthetic and non-functional aspect. In addition, numerous tests have been carried out to determinate the optimal values of nozzle and print bed temperatures that did not lead to problems of warping or delamination. The final choice stands at 225 °C for the nozzle and 75 °C for the print bed, hence same values for both. As regards the printing speeds, after some tests, two different values have been selected for the deposition of the first layer and the remaining ones: 20 mm/s and 60 mm/s. Finally, a configuration with two perimeters was adopted to completely fill the material gaps and maintain the right precision at a geometric level. Additionally, 3 mm of brim were used to enhance adhesion to the print bed.

Specimens were tested using a Zwick Roell 10 kN by ZwickRoell GmbH & Co. KG, Ulm [64].

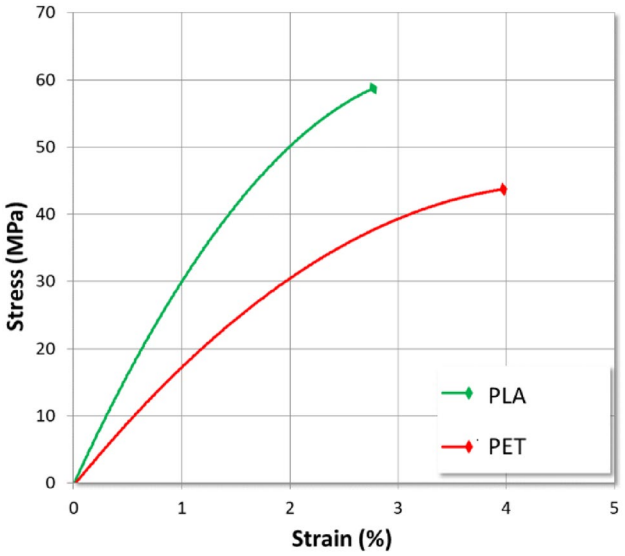

Fig. 4 Tensile test results (mean values) for the UNI EN ISO 527-2:2012 standard 1A DfAM geometry for PLA and PET materials

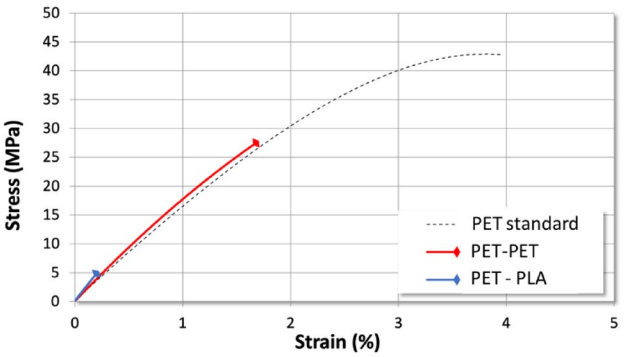

Fig. 5 Comparison of tensile test results (mean values) between the UNI EN ISO 527–2:2012 standard 1A DfAM geometry for PET base material, mono-material and multi-material butt interfaces

4 Results and discussion

In this section the results of the experimental tests are reported and commented in detail.

In Fig. 4 the mean values of the tensile tests on the UNI EN ISO 527–2:2012 standard 1A DfAM geometry are shown. These results set the reference values for the material in mono-material configuration and no interface.

PLA (Fig. 4), young modulus E_{PLA} 3379.1 ± 34.9 MPa, is a slightly stiffer material than the PET (Fig. 4), E_{PET} 1998.5 ± 2.8 MPa, while PET is a tougher material as it shows an elongation at break of 3.87 ± 0.42% and PLA shows an elongation at break of 2.77 ± 0.04%.

The effect of the existence of the interface is assessed using the butt configuration (Fig. 5).

The interface in mono-material configuration has a relevant effect as it almost halve the mechanical properties of the specimen, the Ultimate Tensile Strength (UTS) decrease from 44.3 ± 1.3 MPa for PET standard to 27.3 ± 1.4 MPa for mono-material, while in the multi-material configuration there is a dramatic effect as the values are around a tenth of the standard geometry (4.8 ± 0.9 MPa). An explanation can be drawn observing the failure surfaces reported in Fig. 6.

In Fig. 6 the failure surfaces of the mono-material PLA-PLA (Fig. 6a) show some light gray material on the dark gray one (on the left side). Also the failure surfaces of mono-material PET-PET (Fig. 6b) show some red material on the white one (on the right side), while the failure surfaces of the multi-material PET-PLA (Fig. 6c) show clean surfaces, suggesting weak adhesion between the materials.

In Fig. 7a and b the effect of the geometry on the mechanical properties is assessed performing tensile tests of the PLA and PET mono-materials specimens.

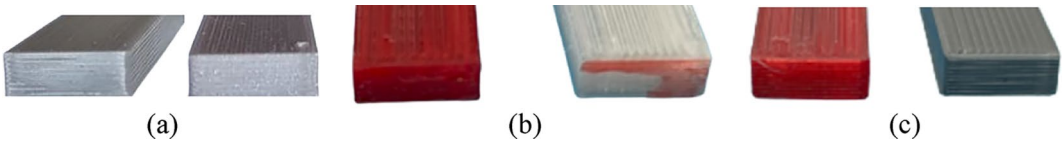

Fig. 6 Detail of the typical failure surfaces of the mono-material PLA-PLA (**a**), mono-material PET-PET (**b**) and multi-material PET-PLA (**c**) butt interfaces

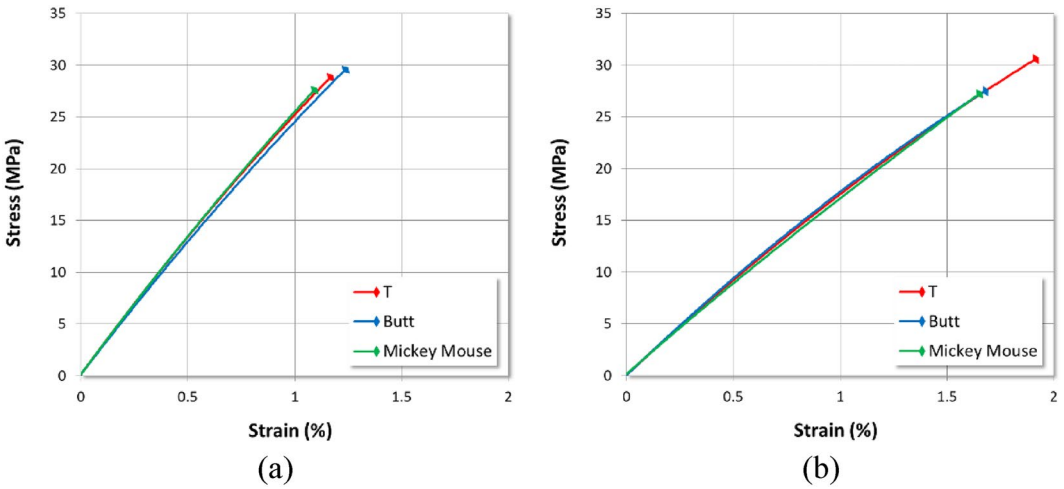

Fig. 7 Comparison of tensile test results (mean values) between the interfaces for the PLA (**a**) and PET (**b**) mono-material interfaces

Table 1 UTS values, mean and standard deviation, of the all mono-material investigated configurations

	PLA		PET	
	UTS (MPa)		UTS (MPa)	
	Mean	Std deviation	Mean	Std deviation
T	28.6	3.8	30.2	0.7
Butt	29.5	5.5	27.3	1.4
MM	27.5	3.0	26.9	2.7

The results do not show relevant variation as shown in Table 1. And all the failure surfaces (Figs. 6a, 8) have inter-interface pattern that highlight strong adhesion.

The tensile test results of the interfaces for the PET-PLA multi-material specimens are reported in Fig. 9 for T interface and in Fig. 10 for MM interface.

It can be observed that after the elastic zone of the curves the behaviors are completely different, with T interface exhibiting a brittle failure (Fig. 9), while the MM interface

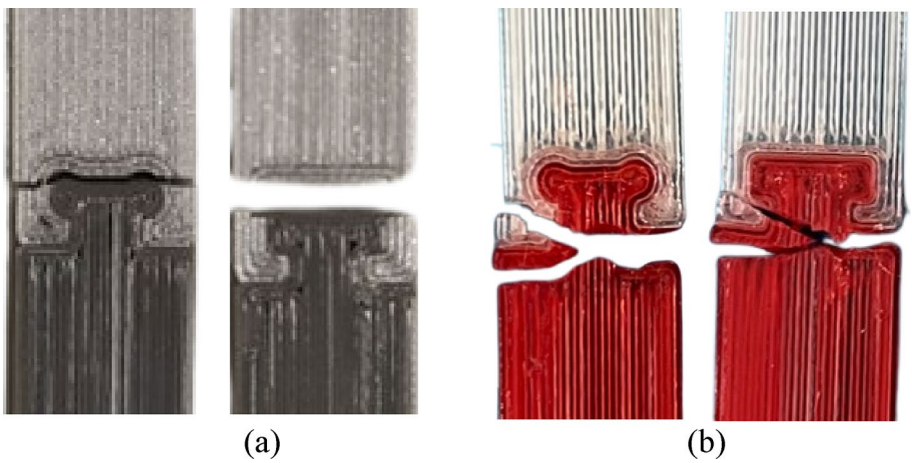

Fig. 8 Detail of the typical failure surfaces of the mono-material PLA-PLA (**a**) and PET-PET (**b**) with MM and T interfaces respectively

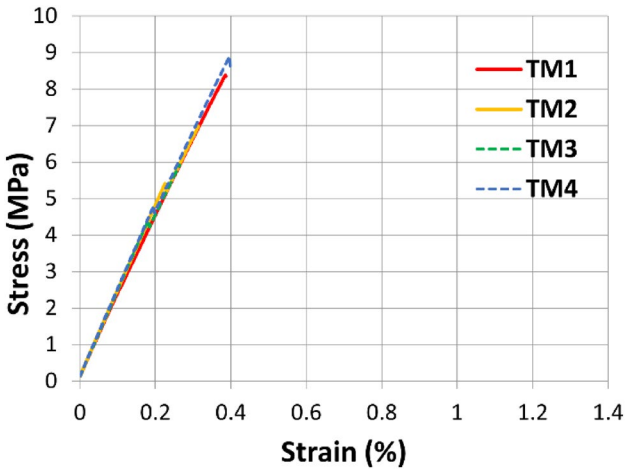

Fig. 9 Tensile test results, for each repetition, of the T interface for the PET-PLA multi-material specimens (reported as TM and repetition number in the legend)

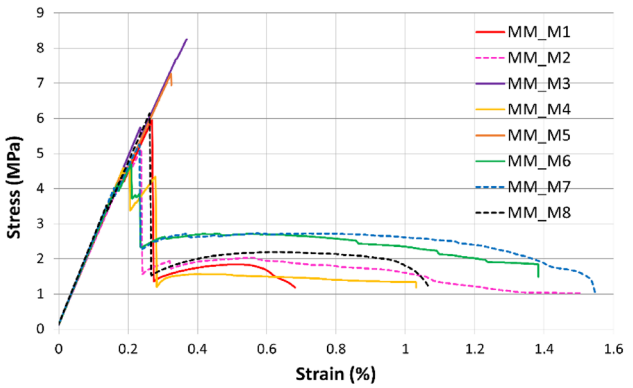

Fig. 10 Tensile test results, for each repetition, of the MM interface for the PET-PLA multi-material specimens (reported as MM_M and repetition number in the legend)

(Fig. 10) has residual strength and deformation capability after a first partial failure.

Explanation can be drawn observing the failure surfaces in Fig. 11 and the failure evolution during the tension tests (Fig. 12).

In Fig. 11b can be observed that the failure occurs almost instantly in the male part (PET) after the detach of short and transversal to the load interface between the different materials due to the locking geometry. In Figs. 11a and 12 is depicted how the lobate geometry allow a gradual failure after the detach of short and transversal to the load interface establishing a rotation pivot for the female part (PLA) on the male part. After an initial interfacial separation where there is an equivalent butt joint interface, approximately at 0.1% of deformation, the load bearing capability of the overall MM interface is guaranteed by the interlocking effect.

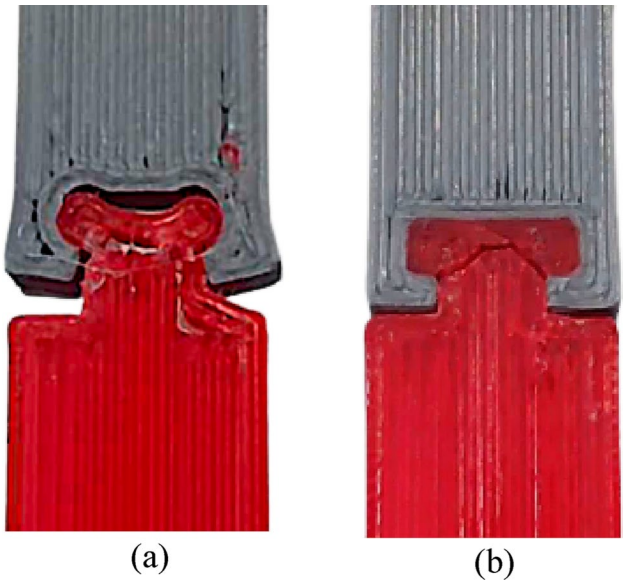

Fig. 11 Detail of the typical failure surfaces of the multi-material PET-PLA MM (**a**) and T (**b**) interfaces

Approximately at 0.25% the female part rotation mechanism allows sliding up to the male part failure. The final failure, transversal to the filament orientation as depicted in Fig. 11, occurs in the minimum cross section of the male part that was designed maintaining the dimensions and the depositions parameters.

The different local failure mechanisms are the cause of the different overall mechanical properties in terms of ultimate strength (Figs. 13 and 14) and total deformation (Fig. 15).

Therefore it can be seen (Figs. 13 and 14) that in terms of ultimate strength the T interface has always the best performance and almost doubling the butt and MM interfaces performances in the multi-material configurations.

In terms of total deformation there are no relevant differences in the mono-material configurations (Fig. 7) while in the multi-material configuration the MM outperform the other interfaces (Fig. 15).

According to the results reported in [65] switching the materials of the sub-parts, i.e. having a stiffer male sub-part, would not modify the trends but would decrease the load bearing and would increase the deformation capability of the studied interfaces.

5 Conclusions

In this study, mono-material specimens, both with and without a boundary interface, along with multi-material specimens, were designed and manufactured using the polymeric filament additive manufacturing. The impact of the presence

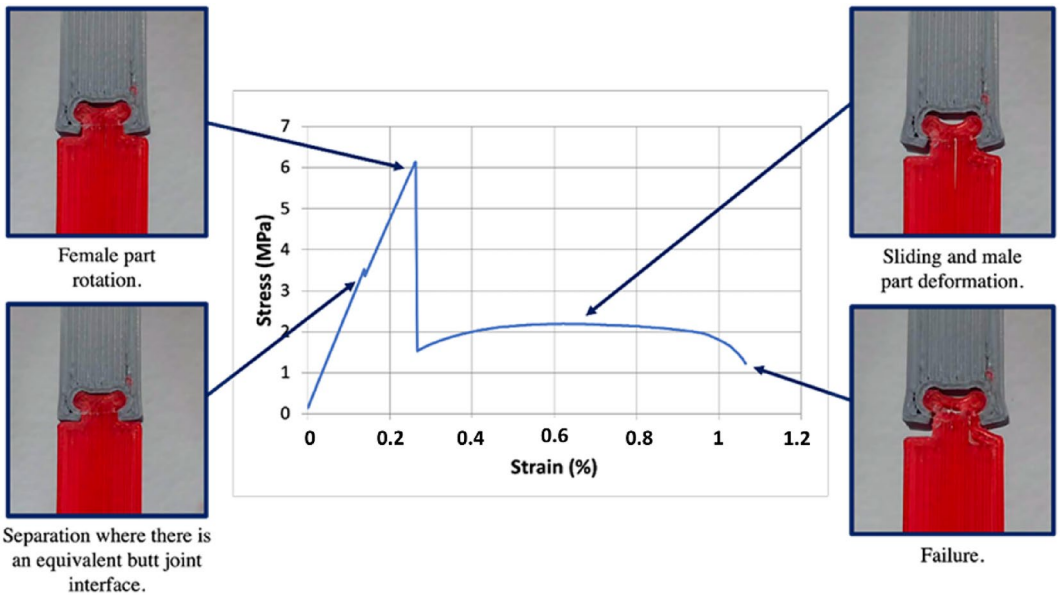

Fig. 12 Analysis of a typical deformation and failure behavior of the MM multi-material interface

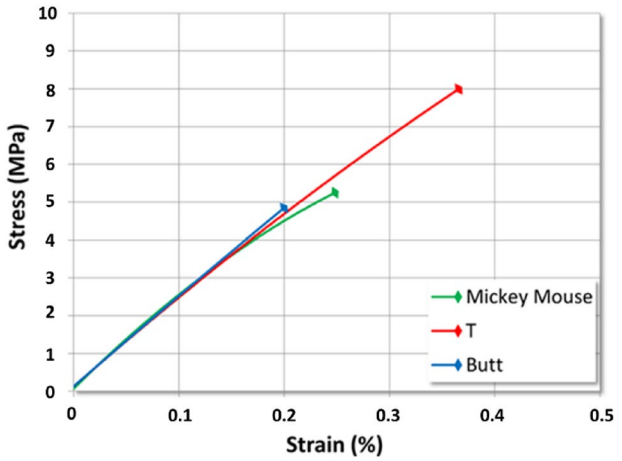

Fig. 13 Comparison of tensile test results (mean values) at ultimate strength between the PET-PLA multi-material interfaces

of the boundary interface and the specific geometries on the structural integrity of the specimens was assessed and analysed, confirming that the interface, both in mono-material and multi-material configuration, has a non-negligible effect that should be considered in DfAM. For example, in the conductive composite for embedded circuits applications, it is convenient to use as matrix the same material of the bulk used to manufacture the component. Mechanical properties of the specimens were systematically investigated and discussed conducting a qualitative failure surfaces analysis, confirming that the chemical affinity prevails over the effect of the mechanical interface.

The key findings are:

- T shape maximise the ultimate strength mechanical property due to its locking effect. Referring to the ultimate tensile strength of the standard ISO 527–2 specimen, the butt interface yield at a residual strength of 60% for homogeneous materials but only 10% for heterogene-

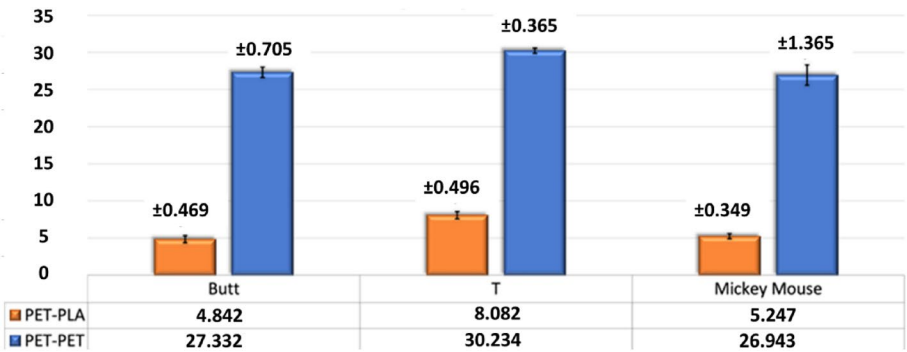

Fig. 14 Ultimate strength (MPa), standard deviation reported as error bar on top, overall comparison for the investigated interfaces

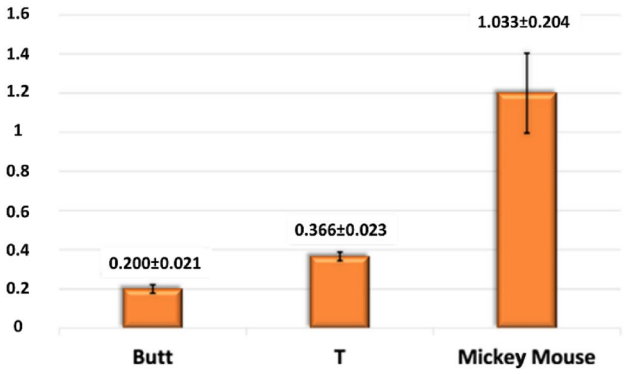

Fig. 15 Total deformation (%), standard deviation reported as error bar on top, comparison for the multi-material PET-PLA configurations

ous materials. The negative effect of the heterogeneous materials configuration was mitigated by the interfaces, resulting in improvements of 7% and 58% for the Mickey Mouse and T geometries, respectively, compared to the butt geometry.

- MM shape maximise the total deformation mechanical property due to its rotation-and-slide effect. Using the total deformation of the standard ISO 527–2 specimen as reference the butt interface elongation at break value decreases of 60% and 95% in the mono-material and in the multi-material configuration respectively. While in the mono-material configuration the elongation at break values are little affected by the interface, in the multi-material configuration the elongation at break values increase of 183% and 516% for the Mickey Mouse and T geometries, respectively, compared to the butt geometry.

Taking into accounts that Mickey Mouse geometry was introduced to decrease stress concentrations around sharp edges, it was possible to observe that the type of fracture has validated the hypothesis at the base since the specimens did not break in the vicinity of the critical points. On the other hand, it did not satisfy this research's primary aim of finding a method that increases multi-material adhesion since the tensile strength was not as high as the one encountered with the T shape of reference.

It is worth noting that these are preliminary results, i.e., the MM shape dimensioning was not optimized, and that different materials combinations could have different trends depending on the chemical affinity and the stiffness mismatch, that need further investigations to be generalized. In particular, in order to completely profit from the new geometry, a design optimization is still logically needed. This is mainly because in this investigation the dimensions of the MM shape have been defined from the adaptation of those of the T one. However, as demonstrated, the two interfaces show different behaviours, consequently it seems correct to carry out an appropriate sizing of the new proposed geometry to stand out and optimize its properties. One of the potential improvements could be to work on finding the correct proportion of Mickey Mouse's "ears". In fact, these are the part of the geometry that allows the blocking of the joint during a tensile test and if correctly sized they could allow to increase the overall strength.

Funding Open access funding provided by Università degli Studi di Genova within the CRUI-CARE Agreement.

Data availability All data generated or analysed during this study are included in this published article.

Declarations

Conflict of interest All authors certify that they have no affiliations with or involvement in any organization or entity with any financial interest or non-financial interest in the subject matter or materials discussed in this manuscript.

References

1. Parvanda R, Kala P (2023) Trends, opportunities, and challenges in the integration of the additive manufacturing with industry 4.0. Prog Addit Manuf 8(3):587–614
2. Nazir A, Gokcekaya O, MdMasumBillah K, Ertugrul O, Jiang J, Sun J et al (2023) Multi-material additive manufacturing: a systematic review of design, properties, applications, challenges, and 3D printing of materials and cellular metamaterials. Mater Des 226:111661
3. Marques A, Cunha A, Gasik M, Carvalho O, Silva FS, Bartolomeu F (2023) 3D multi-material laser powder bed fusion: Ti6Al4V–CuNi2SiCr parts for aerospace applications. Prog Addit Manuf. https://doi.org/10.1007/s40964-023-00460-5
4. Bergonzi L, Pirondi A, Moroni F, Frascio M, Avalle M (2021) A study on Fused Filament Fabrication (FFF) parameters as bonded joint design factors. J Adhes. https://doi.org/10.1080/00218464.2020.1862655
5. Frascio M, Mandolfino C, Moroni F, Jilich M, Lagazzo A, Pizzorni M et al (2021) Appraisal of surface preparation in adhesive bonding of additive manufactured substrates. Int J Adhes Adhes 106:102802
6. Frascio M, André E, Marques DS, João R, Carbas C (2020) Review of tailoring methods for joint with additively

manufactured adherends and adhesives. Materials. https://doi.org/10.3390/ma13183949
7. Frascio M, Moroni F, Marques E, Carbas RJC, dos Reis MQ, Monti M et al (2021) Feasibility study on hybrid weld-bonded joints using additive manufacturing and conductive thermoplastic filament. J Adv Join Process. https://doi.org/10.1016/j.jajp.2021.100046
8. Silva LRR, Marques EAS, da Silva LFM (2021) Polymer joining techniques state of the art review. Weld World 65(10):2023–2045
9. Khatoon S, Khandelwal A, Raj A, Ahmad G (2023) Fabrication of FFF 3D-printed surfaces for PMMA-based biomedical device employing the pre-processing optimization to eliminate the post-processing steps. Prog Addit Manuf. https://doi.org/10.1007/s40964-023-00497-6
10. Launey ME, Buehler MJ, Ritchie RO (2010) On the mechanistic origins of toughness in bone. Annu Rev Mater Res 40(1):25–53
11. Yang W, Quan H, Meyers MA, Ritchie RO (2019) Arapaima fish scale: one of the toughest flexible biological materials. Matter 1(6):1557–1566
12 Marques JB, Barbosa AQ, da Silva CI, Carbas RJC, da Silva LFM (2019) An overview of manufacturing functionally graded adhesives–challenges and prospects. J Adhesion. https://doi.org/10.1080/00218464.2019.1646647
13. dos Reis MQ, Marques EAS, Carbas RJC, da Silva LFM (2020) Functionally graded adherends in adhesive joints: an overview. J Adv Join Process 2:100033
14. Heitkamp T, Kuschmitz S, Girnth S, Marx JD, Klawitter G, Waldt N et al (2023) Stress-adapted fiber orientation along the principal stress directions for continuous fiber-reinforced material extrusion. Prog Addit Manuf 8(3):541–559
15. Zaheri A, Fenner JS, Russell BP, Restrepo D, Daly M, Wang D et al (2018) Revealing the mechanics of helicoidal composites through additive manufacturing and beetle developmental stage analysis. Adv Funct Mater. https://doi.org/10.1002/adfm.201803073
16 Ning H, Flater P, Gaskey B, Gibbons S (2023) Failure mechanisms of 3D printed continuous fiber reinforced thermoplastic composites with complex fiber configurations under impact. Prog Addit Manuf. https://doi.org/10.1007/s40964-023-00479-8
17. Sharafi S, Santare MH, Gerdes J, Advani SG (2021) A review of factors that influence the fracture toughness of extrusion-based additively manufactured polymer and polymer composites. Addit Manuf 38:101830
18. Díaz-Rodríguez JG, Pertúz-Comas AD, González CJA, López DDG, Hernández WP (2023) Monotonic crack propagation in a notched polymer matrix composite reinforced with continuous fiber and printed by material extrusion. Prog Addit Manuf 8(4):733–744
19. Ikram H, Al Rashid A, Koç M (2022) Additive manufacturing of smart polymeric composites: Literature review and future perspectives. Polym Compos 43(9):6355–6380
20. Memarzadeh A, Safaei B, Tabak A, Sahmani S, Kizilors C (2023) Advancements in additive manufacturing of polymer matrix composites: a systematic review of techniques and properties. Mater Today Commun 36:106449
21. Kuzmanić I, Vujović I, Petković M, Šoda J (2023) Influence of 3D printing properties on relative dielectric constant in PLA and ABS materials. Prog Addit Manuf 8(4):703–710
22 Glogowsky A, Korger M, Rabe M (2023) Influence of print settings on conductivity of 3D printed elastomers with carbon-based fillers. Prog Addit Manuf. https://doi.org/10.1007/s40964-023-00483-y
23. de Faria JVG, Pontes LM, Bomfim CC, Ciuffi KJ, Rocha LA, Nassar EJ et al (2023) Incorporation of silver nanoparticles into polyamide powder for application in 3D printing. Prog Addit Manuf. https://doi.org/10.1007/s40964-023-00410-1
24 Flowers PF, Reyes C, Ye S, Kim MJ, Wiley BJ (2017) 3D printing electronic components and circuits with conductive thermoplastic filament. Addit Manuf 18(2017):156–63. https://doi.org/10.1016/j.addma.2017.10.002
25. Baldini G, Staiano M, Grella F, Frascio M, Maiolino P, Cannata G (2023) Mathematical model and experimental characterization of vertically stacked capacitive tactile sensors. IEEE Sens J 23(18):21341–21354
26. Stano G, Di Nisio A, Lanzolla A, Percoco G (2020) Additive manufacturing and characterization of a load cell with embedded strain gauges. Precis Eng 62:113–20. https://doi.org/10.1016/j.precisioneng.2019.11.019
27 Cerbe F, Mahlstedt D, Sinapius M, Hühne C, Böl M (2023) Relationship between programming stress and residual strain in FDM 4D printing. Prog Addit Manuf. https://doi.org/10.1007/s40964-023-00477-w
28 Kumar P, Dwivedy SK, Banerjee S (2023) Fabrication and experimental characterizations of smart material filaments (SMFs) for possible future 4D-printing applications. Prog Addit Manuf. https://doi.org/10.1007/s40964-023-00467-y
29 Ladakhan SH, Sreesha RB, Adinarayanappa SM (2023) A study of the functional capabilities of shape memory alloy-based 4D printed analogous bending actuators. Prog Addit Manuf. https://doi.org/10.1007/s40964-023-00456-1
30. Klahn C, Singer D, Meboldt M (2016) Design guidelines for additive manufactured snap-fit joints. Procedia CIRP 50:264–269
31. Golewski P, Sadowski T (2023) Application of Thermo-Bimaterial Effect in Designing of Snap-Fit Joints. Arch Metall Mater. https://doi.org/10.24425/amm.2019.129499
32. Avalle M, Monti M, Frascio M (2023) Modeling the strength of laminated parts made by fused filament fabrication additive manufacturing. Proc Inst Mech Eng C J Mech Eng Sci 20:095440622311614
33. Croccolo D, De Agostinis M, Olmi G (2013) Experimental characterization and analytical modelling of the mechanical behaviour of fused deposition processed parts made of ABS-M30. Comput Mater Sci 79:506–18
34. Seibert P, Susmel L, Berto F, Kästner M, Razavi N (2021) Applicability of strain energy density criterion for fracture prediction of notched PLA specimens produced via fused deposition modeling. Eng Fract Mech 258:108103
35. Jilich M, Frascio M, Avalle M, Zoppi M (2019) Development of a gripper for garment handling designed for additive manufacturing. Proc Inst Mech Eng C J Mech Eng Sci. https://doi.org/10.1177/0954406219857763
36. Frascio M, Jilich M, Pizzorni M, Monti M, Avalle M, Zoppi M (2019) The use of low pressure plasma surface modification for bonded joints to assembly a robotic gripper designed to be additive manufactured. Procedia Struct Integr 24:204–12. https://doi.org/10.1016/j.prostr.2020.02.017
37. Hasanov S, Alkunte S, Rajeshirke M, Gupta A, Huseynov O, Fidan I et al (2021) Review on additive manufacturing of multi-material parts: progress and challenges. J Manuf Mater Process 6(1):4
38. Nazir A, Gokcekaya O, MdMasumBillah K, Ertugrul O, Jiang J, Sun J et al (2023) Multi-material additive manufacturing: a systematic review of design, properties, applications, challenges, and 3D printing of materials and cellular metamaterials. Mater Des 226:111661
39. Cunha P, Teixeira R, Carneiro OS, Silva AF (2023) Multi-material fused filament fabrication: an expedited methodology to assess the affinity between different materials. Prog Addit Manuf 8(2):195–204

40. Yin J, Lu C, Fu J, Huang Y, Zheng Y (2018) Interfacial bonding during multi-material fused deposition modeling (FDM) process due to inter-molecular diffusion. Mater Des 150:104–112
41. Ribeiro M, Sousa Carneiro O, Ferreira da Silva A (2019) Interface geometries in 3D multi-material prints by fused filament fabrication. Rapid Prototyp J 25(1):38–46
42 da Silva LFM, Öchsner A, Adams RD (eds) (2018) Handbook of adhesion technology. Springer International Publishing, Cham. https://doi.org/10.1007/978-3-319-55411-2
43. Ermolai V, Sover A, Boca MA, Hriţuc A, Slătineanu L, Nagîţ G et al (2022) Mechanical behaviour of macroscopic interfaces for 3D printed multi-material samples. MATEC Web of Conf 19(368):01004
44. Dairabayeva D, Perveen A, Talamona D (2023) Investigation on the mechanical performance of mono-material vs multi-material interface geometries using fused filament fabrication. Rapid Prototyp J 29(11):40–52
45. Andó M, Birosz M, Jeganmohan S (2021) Surface bonding of additive manufactured parts from multi-colored PLA materials. Measurement 169:108583
46. Sun X, Mazur M, Cheng CT (2023) A review of void reduction strategies in material extrusion-based additive manufacturing. Addit Manuf 67:103463
47 Sherugar S, Birkett M, Blacklock M (2023) Characterisation of print path deviation in material extrusion. Prog Addit Manuf. https://doi.org/10.1007/s40964-023-00502-y
48. Zafferani Glas (2023) Zafferani Glas Company, p 1–1. https://zafferani.com. Accessed 27 Dec 2023
49. PRUSA (2023) PRUSA. https://www.prusa3d.com/. Accessed 27 Dec 2023
50. Slotwinski J, Moylan S. Applicability of Existing materials testing standards for additive manufacturing materials. Gaithersburg, MD; 2014 Jun.
51. ICE filaments (2023) ICE filaments. https://icefilaments.com/. Accessed 27 Dec 2023
52. SUNLU (2023) SUNLU. https://www.sunlu.com/. Accessed 27 Dec 2023
53. Lopes LR, Silva AF, Carneiro OS (2018) Multi-material 3D printing: the relevance of materials affinity on the boundary interface performance. Addit Manuf 23:45–52
54. Atakok G, Kam M, Koc HB (2022) Tensile, three-point bending and impact strength of 3D printed parts using PLA and recycled PLA filaments: a statistical investigation. J Market Res 18:1542–1554
55. Mercado-Colmenero JM, La Rubia MD, Mata-Garcia E, Rodriguez-Santiago M, Martin-Doñate C (2020) Experimental and numerical analysis for the mechanical characterization of PETG polymers manufactured with FDM technology under pure uniaxial compression stress states for architectural applications. Polymers (Basel) 12(10):2202
56 Croccolo D, De Agostinis M, Fini S, Mele M, Olmi G, Campana G (2023) Effects of infill temperature on the tensile properties and warping of 3D-printed polylactic acid. Prog Addit Manuf. https://doi.org/10.1007/s40964-023-00492-x
57. Bruère VM, Lion A, Holtmannspötter J, Johlitz M (2023) The influence of printing parameters on the mechanical properties of 3D printed TPU-based elastomers. Prog Addit Manuf 8(4):693–701
58 Birosz MT, Andó M (2023) Effect of infill pattern scaling on mechanical properties of FDM-printed PLA specimens. Prog Addit Manuf. https://doi.org/10.1007/s40964-023-00487-8
59 Golbabapour S, Kabir MZ (2023) Material characterization and micro-damage detection of additive manufactured poly-lactic-acid products using material extrusion-based technique. Prog Addit Manuf. https://doi.org/10.1007/s40964-023-00461-4
60 Zirak N, Benfriha K, Shakeri Z, Shirinbayan M, Fitoussi J, Tcharkhtchi A (2023) Interlayer bonding improvement and optimization of printing parameters of FFF polyphenylene sulfide parts using GRA method. Prog Addit Manuf. https://doi.org/10.1007/s40964-023-00469-w
61. Pereira RBD, Pereira EB, Oliveira PR, Christoforo AL, del Pino GG, Panzera TH (2023) The effect of printing parameters on the tensile properties of bidirectional PLA structures: a statistical approach. Prog Addit Manuf 8(3):519–527
62 CaptanPrabakaran A, Senthil P, Sathies T (2023) Experimental and numerical investigations on the fatigue characteristics of FFF-printed acrylonitrile styrene acrylate parts. Prog Addit Manuf. https://doi.org/10.1007/s40964-023-00432-9
63 Kiendl J, Gao C (2020) Controlling toughness and strength of FDM 3D-printed PLA components through the raster layup. Compos B Eng. 180:107562. https://doi.org/10.1016/j.compositesb.2019.107562
64. Zwick-Roell. Zwick-Roell 3D printed robotic end effector for material testing. https://www.zwickroell.com/en/automated-testing-systems/robotest-n-smart-light-weight-robot. Accessed 27 Dec 2023
65. Mihalache AM, Ermolai V, Sover A, Nagîț G, Boca MA, Slătineanu L et al (2022) Tensile behavior of joints of strip ends made of polymeric materials. Polymers (Basel) 14(22):4990